Carbon 114 (2017) 700–705

Contents lists available at ScienceDirect

Carbon

journal homepage: www.elsevier.com/locate/carbon

Systematic evaluation of different types of graphene oxide in respect to variations in their in-plane modulus

Patrick Feicht [a], Renée Siegel [b], Herbert Thurn [c], Jens W. Neubauer [d], Maximilian Seuss [d], Tamás Szabó [e], Alexandr V. Talyzin [f], Christian E. Halbig [g], Siegfried Eigler [h], Daniel A. Kunz [a], Andreas Fery [d, i], Georg Papastavrou [j], Jürgen Senker [b], Josef Breu [a, *]

[a] Lehrstuhl für Anorganische Chemie I, University of Bayreuth, Universitätsstraße 30, 95440 Bayreuth, Germany
[b] Lehrstuhl für Anorganische Chemie III, University of Bayreuth, Universitätsstraße 30, 95440 Bayreuth, Germany
[c] Computing Center, University of Bayreuth, Universitätsstraße 30, 95440 Bayreuth, Germany
[d] Institute for Physical Chemistry and Polymer Physics, Leibniz-Institut für Polymerforschung Dresden e.V., 01069 Dresden, Germany
[e] Department of Physical Chemistry and Materials Science, University of Szeged, Aradi vertanuk tere 1, H-6720 Szeged, Hungary
[f] Department of Physics, Umeå University, SE-901 87 Umeå, Sweden
[g] Lehrstuhl für Organische Chemie II, FAU Erlangen-Nürnberg, 90762 Fürth, Germany
[h] Chemistry and Chemical Engineering, Chalmers University of Technology, 412 96 Gothenburg, Sweden
[i] Chair of Physical Chemistry of Polymeric Materials, Technical University Dresden, 01069 Dresden, Germany
[j] Lehrstuhl für Physikalische Chemie II, University of Bayreuth, Universitätsstraße 30, 95440 Bayreuth, Germany

ARTICLE INFO

Article history:
Received 25 October 2016
Received in revised form
14 December 2016
Accepted 24 December 2016
Available online 28 December 2016

ABSTRACT

Graphene oxide samples prepared in various laboratories following a diversity of synthesis protocols based on Brodie's (BGO) and Hummers/Offeman's (HGO) methods were compared in respect of their in-plane moduli. A simple wrinkling method allowed for a spatial resolution <1.5 μm by converting the wrinkling frequency. Quite surprisingly, a drastic variation of the in-plane moduli was found spanning the range from 600 GPa for the best BGO types, which is in the region of chemically derived graphene, all the way down to less than 200 GPa for HGO types. This would suggest that there are no two equal GO samples and GO should not be regarded a compound but rather a class of materials with very variable physical properties. While large differences between Brodie's and Hummers/Offeman's types might have been expected, even within the group of Hummers/Offeman's types pronounced differences are observed that, based on ^{13}C solid-state NMR, were related to over-functionalization versus over-oxidation.

1. Introduction

In the note of B. C. Brodie in 1855 [1] about the purification of graphite he described the first preparation of graphene oxide (GO). Since then, essentially two other preparation methods were established by Staudenmaier in 1899 [2] and Hummers/Offeman in 1958 [3], similarly described by Charpy in 1909 [4]. Nowadays, the Hummers/Offeman method is commonly used because it is faster and safer than the others. The structure of GO is still a big puzzle, as it is a heterogeneous and turbostratically disordered material with varying amounts and types of functional groups. Moreover, the proposed structure models are based on GO prepared by different synthesis methods [5–9]. All synthesis protocols apply quite harsh conditions, such as concentrated acids and strong oxidizing agents, for the oxidation of graphite. Due to the heterogeneous character of the oxidation reaction and the fact that an electronic conductor (graphite) is converted into an insulator (GO) in the course of the reaction, gradients in the local concentration of the reactants are inherent to the process. Accordingly, the type, number and density of functional groups (hydroxyl, epoxy, carboxyl, organosulfates) [8,9] introduced by oxidation vary spatially within the material and, moreover, critically depend on the kinetics of the reaction and on the reactants used. As the oxidation starts at the rim of the platelets and concentrically proceeds to the geometric center, defects will be created by local over-oxidation to CO_2. The size and therefore the size distribution of the type of graphite used also determines the degree of over-oxidation [10]. A degradation of the smaller platelets will commence while the larger ones are not yet completely

* Corresponding author.
E-mail address: josef.breu@uni-bayreuth.de (J. Breu).

http://dx.doi.org/10.1016/j.carbon.2016.12.065
0008-6223/

converted to GO. Consequently, the properties of GO vary for every batch which was prepared by even the same synthesis protocol. Kunz et al. found that there are even variations within sub-μm domains of a single nanoplatelet [11].

The choice of reactants also changes the intracrystalline reactivity of GO. Strong differences of swelling behavior of different types of GO are well established. BGO typically exhibits crystalline swelling and phase transitions between one and two layered solvates, while HGO shows osmotic swelling in all so far studied solvents [12–14].

Typically, GO is characterized by X-ray diffraction, NMR and vibrational spectroscopy and local variations are consequently averaged in the bulk analysis [15]. Rare exceptions are X-ray photoelectron spectroscopy and μm-Raman spectroscopy that allow for determination of functional groups and defect densities of reduced GO in the μm range [16,17].

Recently, we presented a characterization of the mechanical properties of HGO and chemically reduced HGO sheets with high spatial resolution by applying a simple wrinkling procedure [11]. Herein, we apply this method to compare graphene oxide samples prepared in various laboratories following a diversity of synthesis protocols (supporting information) based on Brodie's (BGO) and Hummers/Offeman's (HGO) methods in respect of their in-plane moduli.

2. Experimental

Topographic AFM images were obtained using two different commercial AFM instruments, a Nanoscope Dimension V and ICON AFM from Bruker, USA, operated in TappingMode™. Aluminum-coated silicon cantilevers (OTESPA-R3, Bruker) with a spring constant of 26 N m^{-1} and typical resonance frequencies of 300 kHz were used. Image processing and analysis was conducted with NanoScope Analysis v1.40.

All ^{13}C MAS solid-state NMR experiments were acquired on Bruker Avance-III HD spectrometers operating at a B0 field of 9.4 T, corresponding to a ^{13}C and ^{1}H frequency of 100.6 MHz and 400.1 MHz, respectively. The samples were spun at 12.5 kHz in a 4 mm MAS double resonance probe (Bruker). The one-pulse MAS spectra were obtained after 160–440 scans using a 90° pulse of 3.5 μs and a recycle delay of 360 s. Proton broadband decoupling of 70 kHz with spinal-64 was applied during acquisition. All ^{13}C spectra are referenced with respect to tetramethylsilane using the secondary standard adamantane. Deconvolution of NMR spectra.

TopSpin 3.2 was used for the deconvolution of the NMR spectra. A range from 380 ppm to −110 ppm was used. The Gauss/Lorentz ratio was kept constant at 0.5 and 7000 iterations were made. Linebroadening for overlapping peakgroups were tried to be kept in the same range. The best overlaps were above 80%. The integrals of the peaks were normalized to the integral of the peak at 130 ppm.

The degree of functionalization was taken as the ratio of the sum of sp3 signals (60 ppm and 70 ppm) and the sum of all ^{13}C signals.

Raman spectroscopic studies were done on Horiba HR Evolution confocal Raman spectrometer equipped with a microscope (100× objective) and an automated XYZ table, at laser excitation of 532 nm.

3. Synthesis of graphene oxide (GO) samples

3.1. Hummers/Offeman method

3.1.1. HGO Eigler

Natural flake graphite (1 g, 300–425 μm, grade 3061, Asbury Carbon USA) was stirred in cold H_2SO_4 (24 mL, 98 vol%, Sigma Aldrich) for 1 h before $KMnO_4$ (2 g, Sigma Aldrich) were added over 4 h. The mixture was further stirred for 16 h. Then, diluted H_2SO_4 (20 mL, 20 vol%, Sigma Aldrich) was slowly added over 2 h and double distilled water (100 mL) over 16 h. Finally, the reaction was stopped by the addition of H_2O_2 solution over 40 min (40 mL, 5 vol %, Sigma Aldrich). The obtained HGO was purified by repetitive centrifugation and redispersion with pure water (10 min, 1500 RCF). As the pH was almost neutral, delamination was performed by pulsed tip sonication (2 min, 40 W). At last, non-monolayer and minor amounts of smallest particles were removed by repetitive centrifugation at low rpm and then high centrifugation parameters (3 times, 30 min, 1500 RCF, 1 time 45 min, 13000 RCF). We obtained a stable golden dispersion containing exclusively HGO monolayer.

3.1.2. HGO Talyzin

Natural graphite powder (1 g, 74 μm, Alfa Aesar) and $NaNO_3$ (1 g, Scharlau) were added in a flask (placed in an ice bath) to concentrated H_2SO_4 (40 mL, 95–97 vol%, Merck). Magnetic stirring of the mixture solution was maintained at each steps of the synthesis procedure. $KMnO_4$ (3 g, VWR) was added very slowly to the solution in order to avoid the increase of temperature above 20 °C. The flask was removed from the ice bath after 2 h and it was then heated in an oil bath at 35 °C for 2 h. After this first heating step, the solution was poured under vigorous stirring on deionized water H_2O (40 mL) in an ice-surrounded flask (instant temperature increase to 98 °C). The solution was heated a second time in an oil bath at 90 °C for 30 min. Subsequently, deionized water (100 mL) and H_2O_2 (6 mL, 30 vol%, Merck) were added under vigorous stirring in order to stop the synthesis reaction. The resulting material was washed 3 times with a HCl solution (20 mL, 10 vol%, Merck), stirred for 30 min and then centrifuged (4400 rpm, 15 min). The HGO sample was next repeatedly washed with deionized water and centrifuged (4400 rpm, 15 min). Once the pH was brought back to neutral, freeze-drying could be carried out on the HGO sample.

3.1.3. HGO Feicht

Natural flake graphite (1 g, 125–250 μm, Reinstflocke (RFL) 99.5, Kropfmühl AG) and $NaNO_3$ (1 g, Sigma Aldrich) were mixed with concentrated H_2SO_4 (30 mL, 98 vol%, Sigma Aldrich). Subsequently, $KMnO_4$ (3 g, Sigma Aldrich) was interspersed over a period of 3 h and the reaction was kept at room temperature for 12 h. Thereafter, the mixture was slowly poured into ice-cooled deionized water (30 mL) and H_2O_2 (30 vol%, Sigma Aldrich) was added until the solution turned golden. GO was purified by repeated washing/centrifugation (3 times, 10 min, 3800 rpm) followed by a dialysis to an ionic conductivity of 2 μS cm^{-1}.

3.1.4. HGO Feicht extracted

A part of the suspension of HGO Feicht was mixed with the same volume of ethanol and 1-dodecylamine (1 g, Sigma-Aldrich). Afterwards, HGO modified with 1-dodecylamine was extracted into diethyl ether and washed with water. For the removal of the 1-dodecylamine the suspension was mixed with an aqueous NaOH/ethanol mixture (50:50, 700 mL, 4 times), stirred for 15 min and then centrifuged (15 min, 10000 rpm). Finally, HGO was washed with water and centrifuged (3 times, 30 min, 10000 rpm).

3.2. Brodie method

3.2.1. BGO Brand/Böhm 1962

This BGO was also used in the publication “Der “Verpuffungspunkt” des Graphitoxids” of H.-P. Böhm in 1965 and was denoted as “GO-Bra.” in the table on page 78 [18]. The preparation was done following the instructions of B.C. Brodie. [19] We translated the original description quite freely without changing the content:

3.2.1.1. Original text [19].. "Die Operation wird, was die Einzelnheiten betrifft, wie folgt ausgeführt. Eine gewisse Menge Graphit wird mit dem dreifachen Gewicht an chlorsaurem Kali innig gemischt, und diese Mischung in eine Retorte gegeben. Eine zur Verflüssigung des Ganzen genügende Menge der stärksten Salpetersaure wird nun hinzugegeben. Die Retorte wird in ein Wasserbad gestellt, und 3 bis 4 Tage lang bei 60 °C erhalten, bis sich keine gelben Dämpfe mehr entwickeln. Die Substanz wird dann in eine große Menge Wasser geschüttet und durch Decantiren bis zur fast völligen Befreiung von Säure und von Salzen ausgewaschen. Sie wird nun im Wasserbad getrocknet, und die Oxydationsoperation unter Anwendung derselben relativen Mengen chlorsaures Kali und Salpetersaure wiederholt, bis keine weitere Veränderung mehr eintritt; dies ist gewöhnlich nach der vierten Oxydation der Fall. Die Substanz wird endlich erst im leeren Raum und dann bei 100 °C getrocknet."

3.2.1.2. Translation. A certain amount of graphite is properly mixed with a triple weight of $KClO_3$. Concentrated HNO_3 is added until the mixture gets suspended. It is then heated to 60 °C for 3–4 days until the development of yellow vapors stops. The substance is then poured into a large amount of water and washed by decantation until almost completely freed from acid and salts. After drying in a beaker in a water bath, the oxidation process is repeated using the same relative amounts of $KClO_3$ and HNO_3 until no further change occurs; This is usually the case after the fourth oxidation. The substance is finally dried in vacuum and then at 100 °C.

3.2.2. BGO Szabo 2nd ox

Natural flake graphite (1 g, 250–500 μm, Reinstflocke (RFL) 99.5, Kropfmühl AG) and $NaClO_3$ (8.5 g) were mixed in a 50 mL round flask placed into an ice-bath. Next, 6 mL of fuming HNO_3 was added from a dropping funnel in 21 min. The obtained dark green thick slurry was left aging overnight at ambient temperature. The loss of HNO_3 due to evaporation was retrieved by adding another portion of acid (4 mL). The slurry was then heated to 60 °C with a steam bath and kept strictly at 60 ± 1 °C for 8 h. Heating rate (<1.5 °C min^{-1}) was controlled carefully to avoid dangerous deflagration. The reaction was terminated by transferring the pasty mixture into 100 mL of distilled water. The diluted suspension was washed with HCl solution (5 times, 20 mL, 3 M) and with copious amounts of distilled water to remove ionic impurities until the supernatant had an electrical conductivity less than 10 μS cm^{-1} (close to that of distilled water). The residual graphite oxide was separated by sedimentation (the smallest particles were discharged) and finally dried at 60 °C. This BGO was oxidized one more time applying exactly the same procedure, except a triple quantity (3 g) of air-dry BGO was used instead of graphite.

3.2.3. BGO Feicht 2nd ox

Natural flake graphite (1 g, 250–500 μm, Reinstflocke (RFL) 99.5, Kropfmühl AG) and $NaClO_3$ (8.5 g) were mixed in a beaker placed into an ice-bath. Next, 12 mL of fuming HNO_3 was added from a dropping funnel in 12 min. The obtained dark green thick slurry was left aging overnight at ambient temperature. The slurry was then heated to 60 °C with a steam bath and kept strictly at 60 ± 1 °C for 3 h. The reaction was terminated by transferring the pasty mixture into 100 mL of distilled water. The diluted suspension was washed with copious amounts of distilled water to remove ionic impurities until the supernatant had an electrical conductivity of less than 10 μS cm^{-1}. The residual BGO was finally dried at 60 °C. This BGO was oxidized one more time applying exactly the same procedure.

3.2.4. BGO Feicht 3rd ox

BGO Feicht 2nd ox was oxidized one more time applying exactly the same procedure as described above.

3.3. Wrinkling

Preparations and data processing were done according to literature [11].

3.3.1. Preparation of substrates

PDMS precursor (Dow Corning Sylgard 184) was mixed in a 10:1 mass ratio of oligomeric base to curing agent, degassed and poured into (60 × 10 × 2) mm^3 Teflon boats. After prehardening for 20 h at room temperature, the samples were post-treated for 2 h at 150 °C. Tensile tests were carried out on an Instron 5565 universal tester with pneumatic clamps and a 100 N load cell (clamping distance 30 mm, strain rate 200 mm min^{-1}, see ISO 37:2005). The Young's moduli are calculated from the initial slope and averaged over 22 different samples.

3.3.2. Preparation of the wrinkles

Firstly, the PDMS substrates were hydrophilized by immersing them in 10 vol% aqueous HCl solution for 16 h, afterwards they were thoroughly washed with Millipore water and dried, as reported in the literature [20]. Care was taken to ensure that the mechanical properties of the surface were not affected by this procedure. The PDMS substrates were uniaxially stretched in a custom-made apparatus [11,21] to a strain of 33%. In the stretched stage a droplet of diluted GO suspension (typically 0.04 mg mL^{-1}) was added to the center and dried gently to obtain samples with isolated nanoplatelets.

3.3.3. Analytical details

In order to obtain the wavelength of the wrinkles, the image data was processed with a discrete 2D Fourier transformation (2D-FT). This was done applying Scilab [22]. The program routine performs the following steps:

- Read matrix of AFM scan (image sizes were 30 × 30 μm with 1024 × 1024 pixel)
- Generate 20 × 20 submatrices
- Conduct 2D-FT for all submatrices
- Integrate within a range of appropriate ky-values
- Normalize to a range of 0–1 within each image
- Plot intensity profiles

From the used intensity profiles all maxima with a normalized intensity above 0.4 were taken into account (for examples see supporting information Figs. S10–S17). Please note that by generating submatrices the original continues signal is cut and new boundaries are created. This can lead to a leakage-effect that is similar to aliasing in signal processing. It can create artificial values in the FT with half and double the wavelength of the original continuous signal (Fig. S13 at 4 kx in the green box). However, a real value with double the wavelength has by definition 4 times the intensity. Therefore, these artificial values can be easily sorted out. We used over 100 values from a single AFM measurement of a sample and did at least two measurements. Only for the sample BGO Brand/Böhm 1962 it was just possible to get one useful measurement because this 54-year-old sample might be contaminated a little over the time with various (non-ionic) substances that prevent wrinkling. For the calculation of the average in-plane modulus for one sample, we combined all values from the single measurements. It is worth to mention that the given error margins represent the variations of the in-plane modulus within a sample

due to structural heterogeneities and not the error of the measurement. Together with the extracted wrinkling wavelength the following values were used to calculate the in-plane moduli:

$E_s = 3.12 \pm 0.09$ MPa.

$\nu_s = 0.5$, see Ref. [20]

$\nu_p = 0.197$, see Ref. [23]

$h = 0.7$ nm, see Ref. [24]

E_s was obtained by averaging the Young's moduli measured from 22 different samples.

4. Results and discussion

For the preparation of HGO [3] graphite is suspended in an excess of concentrated sulfuric acid and $NaNO_3$ is added to trigger the intercalation reaction [25]. Thereafter, $KMnO_4$ is added for the oxidation. The oxidant is constantly available in high concentrations. The predominant functional groups for HGO are hydroxyl, epoxy and organosulfate groups at both sides of the carbon plane and carboxyl groups at the edges and over-oxidized sites [8,26–28]. The most widely accepted structural model for HGO was proposed by Lerf et al. [8]. This model was supplemented by organosulfate groups by Eigler et al. [27]. The acidic groups, especially the organosulfates, contribute to the negative surface charge which enables spontaneous delamination by osmotic swelling in water even at low pH values [28]. By addition of a base to a golden suspension of HGO it turns dark in seconds, which is supposed to be caused by a rearrangement of the functional groups and the conglomeration of aromatic clusters [29,30].

In the Brodie method fuming HNO3 is dropped onto a mixture of graphite and $KClO_3$ ($KClO_3$ can be replaced by $NaClO_3$ to prevent the formation of insoluble $KClO_4$ [31]). Intercalation and oxidation start concomitantly. Only small amounts of the oxidant are locally formed in situ. Therefore, it is commonly believed that the oxidation has to be repeated several times to attain the critical degree of functionalization which is required for its delamination under basic conditions. When samples are functionalized beyond what is needed for delamination we refer to them as being over-functionalized. The most widely accepted model for BGO was proposed by Szabó et al. [9] and includes hydroxyl, epoxy, phenolic and quinone groups. Since there are no highly acidic groups, such as organosulfates, in BGO, the addition of a base is required for the deprotonation which then triggers delamination. The darkening of BGO by the addition of a base is comparatively slow [31].

Since the spatial variation of functional groups in GO samples is linked to the kinetics of the oxidation as discussed above, even small variations of the synthesis protocol within a given method (BGO or HGO) might have significant effects on the GO samples produced. In particular, reaction time, concentration of the reactants and temperature are crucial factors. Therefore, samples from various laboratories were included in the comparison. The selection includes two samples that were oxidized under identical conditions. While HGO Feicht was purified in the ordinary way by dialysis, HGO Feicht extracted is obtained by extraction with the help of 1-dodecylamine [28]. The organic modifier was then removed with NaOH in ethanol. As already mentioned, NaOH is expected to trigger some rearrangement reactions which can also lead to carbon loss as described by Dimiev et al. [32] and a deeply black HGO type is obtained. Moreover, a “historical” sample prepared in the laboratory of H.-P. Böhm in 1962 was included in the selection (BGO Brand/Böhm 1962). This sample was prepared by Brodie's method and most likely was oxidized four times [18].

Since the in-plane modulus drops drastically when oxidizing graphene (~1000 GPa [33,34]), it appears to be a parameter that very sensitively reveals structural changes when going from graphene to GO (compare BGO Feicht 2nd ox, BGO Feicht 3rd ox in Table 1) and consequently subtle structural differences are revealed of various types of GO (compare BGO Szabó 2nd ox, BGO Feicht 2nd ox in Table 1). The changes in the in-plane modulus thereby reflects the degree of rehybridization of the carbon bonds from sp^2 to sp^3, the type of functional group involved in this rehybridization, and also defects in the 2-dimensional lattice related to local over-oxidation.

Functionalization was quantified by the integrals of deconvolved solid-state NMR peaks (see Fig. S1–S8 in supporting information). The degree of functionalization was taken as the ratio of the sum of sp^3 signals and the sum of all ^{13}C signals. According to the literature, the NMR signals at 60 ppm, 70 ppm and 130 ppm are assigned to epoxy, hydroxyl groups, and aromatic carbons, respectively [8]. Organosulfates have isotopic shifts of 60 ppm or 70 ppm and are therefore superimposed on the epoxy- and hydroxyl signals [28]. Although acid/base titrations of GO provided clear evidence for carboxylic acid groups, they amount only to 0.05 wt% [35] which is below detection limit of NMR if the sample is not ^{13}C-enriched [26].

BGO samples are oxidized stepwise and allow identifying a steady decrease of in-plane moduli with progressive oxidation (Table 1; BGO Feicht 2nd ox, BGO Feicht 3rd ox). Surprisingly, the degree of functionalization of the 54-year-old sample (BGO Brand/Böhm 1962) is still high. As it is well known that UV-light can reduce GO by the release of CO_2 accompanied by the creation of over-oxidized sites, a significant decomposition would have been expected over all these years. As expected by the highest number of oxidation steps, the in-plane modulus for this compound was found to be lowest within the BGO samples.

The in-plane moduli for HGO samples are found to be consistently lower than for BGO samples. The oxidation of graphite by the one-step Hummers/Offeman's method is obviously more thorough than by Brodie's method, which can be explained by a higher concentration of oxidizer. This most likely will include both, over-functionalization and over-oxidation. A less defective state of BGO allows to explain an earlier observed crystalline swelling of this material in most solvents (except water) as compared to osmotic swelling of HGO [36]. Moreover, the full-width at half-maximum of the peaks in the ^{13}C solid-state NMR spectra of BGO samples are consistently smaller than for HGO (see Fig. S1–S6 and Table S2 in supporting information) indicating more homogeneous domains of functional groups in BGO. The samples HGO Talyzin and HGO Feicht are consistent with the fact that an increasing degree of functionalization decreases the in-plane modulus. Despite the pronounced difference in optical appearance, the in-plane moduli of HGO Feicht and HGO Feicht extracted are only slightly different (320 GPa and 295 GPa, respectively). However, due to the significantly lower degree of functionalization of HGO Feicht extracted, a significantly higher in-plane modulus would have been expected. The lower in-plane modulus observed, might be related to base-induced rearrangement and CO_2 releasing deoxygenation reactions [32,37] leading to over-oxidized domains.

While BGO and HGO samples largely differ in respect to their in-plane moduli, the degree of functionalization varies by less than 20%. This might suggest that the HGO in-plane moduli are mostly affected by over-oxidized sites.

For HGO Eigler in-plane moduli of GO and μm-Raman measurements (see Fig. S9 in supporting information) for graphene chemically derived of this sample are in contradiction to the above described trend. Raman measurements indicate a rather low defect concentration of <1% [17]. As has, however, been pointed out by Cançado et al. “some defects do not give rise to the D-peak but change other Raman peaks and peak intensities” [16]. Cançado et al., moreover, suggest that Raman spectroscopy should be complemented with other independent probes to gain a more complete

Table 1
Values for the wrinkling wavelength from the 2-dimensionally Fourier transformed AFM-images for different GO samples and the calculated in-plane moduli with their corresponding variances. Additionally, integrals of the deconvolved peaks in the ^{13}C-solid-state NMR measurements of different GO samples are tabulated.

Sample	HGO Talyzin	HGO Feicht	HGO Eigler	HGO Feicht extracted	BGO Szabó 2nd ox	BGO Feicht 2nd ox	BGO Feicht 3rd ox	BGO Brand/ Böhm 1962
Wrinkling wavelength/nm	136 ± 21	132 ± 14	109 ± 11	127 ± 19	160 ± 28	154 ± 19	145 ± 17	128 ± 14
In-plane modulus/GPa	363 ± 163	320 ± 101	189 ± 64	295 ± 133	599 ± 267	534 ± 185	427 ± 155	293 ± 99
Relative standard deviation/%	45	32	34	45	45	35	36	34
Integral δ_{iso} = 130 ppm C aromatic, conjugated double-bond	1.00	1.00	1.00	1.00	1.00	1.00	1.00	1.00
Integral δ_{iso} = 70 ppm Hydroxyl, organosulfate	0.60	0.97	0.78	0.52	0.57	0.54	0.57	0.68
Integral δ_{iso} = 60 ppm Epoxy, organosulfate	1.20	1.50	0.91	0.27	0.97	0.87	1.24	1.41
Degree of functionalization/%	64	71	63	44	62	59	64	68

picture of the nature of defects. In-plane moduli, as presented here, may indeed turn out to be such a powerful independent probe. Moreover, HGO Eigler has a sulfur content of 4.55 wt% according to combustion elemental analysis, therefore the total weight of organosulfate accounts for about 11 wt% which is double the amount of organosulfate in HGO Feicht [27,28]. The investigated functional groups are substantially different due to the much higher amount of organosulfate groups accounting for high local electrostatic repulsion. That observation suggests that types of functional groups also differently alter the in-plane modulus [38–40], leading to a decreased in-plane modulus here. The lowest in-plane modulus of HGO Eigler may consequently be attributed to a combination of defects that are unable to activate the D-band in the Raman process as well as a higher amount of organosulfate groups.

The local variance of the in-plane moduli within a single platelet of GO can be directly visualized via the regularity of the wrinkles in the AFM images (Fig. 1). The wrinkling frequencies can be determined reliably by a Fourier transformation of 1.5 μm × 1.5 μm areas. The mechanical heterogeneity consequently can be pinned down to this spatial resolution. The average in-plane values given in Table 1 and discussed above are based on measuring two independently prepared AFM-samples. For each sample more than 100 in-plane values were extracted, whereas both different areas on the same and on different platelets were taken into account yielding very good statistics.

The pronounced variance of the in-plane moduli reflects the heterogeneity of the GO comprising both functionalization and over-oxidized sites. Increasing the number of functional groups and defects related to over-oxidation will both lower the in-plane modulus. Both the differences in average values and the large variances observed clearly stress that there is no such thing as a GO compound. The mechanical properties significantly scatter at all length scales (within domains on a single platelet, from platelet to platelet in a sample, and even more so between samples prepared with (slightly) different synthesis protocols).

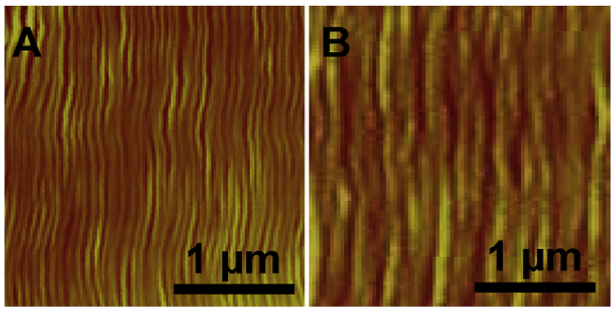

Fig. 1. AFM images of wrinkles with a low variance (A; HGO Eigler) and a high variance (B; BGO Feicht 2nd ox).

5. Conclusion

Since the underlying heterogeneities in the structure of GO are inherent to the oxidation process, a single phase GO material cannot be prepared. Therefore, GO should be rather considered as a class of materials than a component. It can be concluded that statements like “prepared by a modified Hummers/Offeman method” or “oxidized overnight” should not be regarded sufficient. Instead, most detailed descriptions of preparation methods and analysis of chemical functionality are required.

Besides these more general concerns, the remarkably high in-plane modulus of BGO Szabó 2nd ox which is higher than the typical value observed for chemically derived graphene (480 GPa [11]) could make it a superior filler for the mechanical enhancement of water-borne polymer-nanocomposites.

Finally, the simplicity of the wrinkling method renders it suitable for in-process control required to tailor GO synthesis for particular applications.

Acknowledgements

The authors are deeply indebted to Prof. Dr. A. Lerf for providing the “historical” GO sample prepared in the laboratory of Prof. Dr. Hanns-Peter Böhm. Andreas Schedl is gratefully acknowledged for interesting discussions about the PDMS preparation and the support with the tensile test device. P. Feicht would like to thank Christian Kuttner for his support with programming IGOR and Coico for her help making the pictures of the wrinkled samples. T. Szabó and P.Feicht would like to thank the Kropfmühl AG for providing the flake graphite. S.Eigler acknowledges the German Research Council via Grant Nos. EI938/3-1 and SFB953 for financial support.

Appendix A. Supplementary data

Supplementary data related to this article can be found at http://dx.doi.org/10.1016/j.carbon.2016.12.065.

References

[1] B.C. Brodie, Note sur un nouveau procédé pour la purification et la désagrégation du Graphite, Ann. Chim. Phys. 45 (1855) 351–353.
[2] L. Staudenmaier, Verfahren zur Darstellung der Graphitsäure, Ber. Dtsch. Chem. Ges. 31 (1898) 1481–1487.
[3] J. William, S. Hummers, R.E. Offeman, Preparation of graphitic oxide, J. Am. Chem. Soc. 80 (1958) 1339.
[4] G. Charpy, Sur la formation de l'oxyde graphitique et la définition du graphite, C. R. Hebd. Séances Acad. Sci. 148 (1909) 920–923.
[5] U. Hofmann, A. Frenzel, E. Csalán, Die Konstitution der Graphitsäure und ihre Reaktionen, Liebigs Ann. Chem. 510 (1934) 1–41.
[6] G. Ruess, Über das Graphitoxyhydroxyd (Graphitoxyd), Monatsh. Für Chem.

76 (1947) 381–417.
[7] T. Nakajima, A. Mabuchi, R. Hagiwara, A new structure model of graphite oxide, Carbon 26 (1988) 357–361.
[8] A. Lerf, H. He, M. Forster, J. Klinowski, Structure of graphite oxide revisited, J. Phys. Chem. B 102 (1998) 4477–4482.
[9] T. Szabó, O. Berkesi, P. Forgó, K. Josepovits, Y. Sanakis, D. Petridis, et al., Evolution of surface functional groups in a series of progressively oxidized graphite oxides, Chem. Mater. 18 (2006) 2740–2749.
[10] C. Botas, P. Álvarez, C. Blanco, R. Santamaría, M. Granda, P. Ares, et al., The effect of the parent graphite on the structure of graphene oxide, Carbon 50 (2012) 275–282.
[11] D.A. Kunz, P. Feicht, S. Gödrich, H. Thurn, G. Papastavrou, A. Fery, et al., Space-resolved in-plane moduli of graphene oxide and chemically derived graphene applying a simple wrinkling procedure, Adv. Mater. 25 (2013) 1337–1341.
[12] S. You, S.M. Luzan, T. Szabó, A.V. Talyzin, Effect of synthesis method on solvation and exfoliation of graphite oxide, Carbon 52 (2013) 171–180.
[13] A.V. Talyzin, A. Klechikov, M. Korobov, A.T. Rebrikova, N.V. Avramenko, M.F. Gholami, et al., Delamination of graphite oxide in a liquid upon cooling, Nanoscale 7 (2015) 12625–12630.
[14] M.V. Korobov, A.V. Talyzin, A.T. Rebrikova, E.A. Shilayeva, N.V. Avramenko, A.N. Gagarin, et al., Sorption of polar organic solvents and water by graphite oxide: thermodynamic approach, Carbon 102 (2016) 297–303.
[15] B. Rezania, N. Severin, A.V. Talyzin, J.P. Rabe, Hydration of bilayered graphene oxide, Nano Lett. 14 (2014) 3993–3998.
[16] L.G. Cançado, A. Jorio, E.H.M. Ferreira, F. Stavale, C.A. Achete, R.B. Capaz, et al., Quantifying defects in graphene via Raman spectroscopy at different excitation energies, Nano Lett. 11 (2011) 3190–3196.
[17] S. Eigler, M. Enzelberger-Heim, S. Grimm, P. Hofmann, W. Kroener, A. Geworski, et al., Wet chemical synthesis of graphene, Adv. Mater. 25 (2013) 3583–3587.
[18] H.P. Böhm, W. Scholz, Der "Verpuffungspunkt" des Graphitoxids, Z. Anorg. Allg. Chem. 335 (1965) 74–79.
[19] B.C. Brodie, Über das Atomgewicht des Graphits, Ann. Der Chem. Und Pharm. 114 (1860) 6–24.
[20] H. Huang, J.Y. Chung, A.J. Nolte, C.M. Stafford, Characterizing polymer brushes via surface wrinkling, Chem. Mater. 19 (2007) 6555–6560.
[21] M. Pretzl, A. Schweikart, C. Hanske, A. Chiche, U. Zettl, A. Horn, et al., A lithography-free pathway for chemical microstructuring of macromolecules from aqueous solution based on wrinkling, Langmuir 24 (2008) 12748–12753.
[22] http://www.scilab.org/, (n.d.). http://www.scilab.org/.
[23] Q. Peng, S. De, Mechanical properties and instabilities of ordered graphene oxide C6O monolayers, RSC Adv. 3 (2013) 24337.
[24] J.W. Suk, R.D. Piner, J. An, R.S. Ruoff, Mechanical properties of monolayer graphene oxide, ACS Nano 4 (2010) 6557–6564.
[25] W. Rüdorff, U. Hofmann, Über Graphitsalze, Z. Anorg. Allg. Chem. 238 (1938) 1–50.
[26] W. Cai, R.D. Piner, F.J. Stadermann, S. Park, M.A. Shaibat, Y. Ishii, et al., Synthesis and solid-state NMR structural characterization of 13C-labeled graphite oxide, Science 321 (2008) 1815–1817.
[27] S. Eigler, C. Dotzer, F. Hof, W. Bauer, A. Hirsch, Sulfur species in graphene oxide, Chem. A Eur. J. 19 (2013) 9490–9496.
[28] P. Feicht, D.A. Kunz, A. Lerf, J. Breu, Facile and scalable one-step production of organically modified graphene oxide by a two-phase extraction, Carbon 80 (2014) 229–234.
[29] A. Clauss, R. Plass, H.P. Böhm, U. Hofmann, Untersuchungen zur Struktur des Graphitoxyds, Z. Anorg. Allg. Chem. 291 (1957) 205–220.
[30] H.P. Böhm, A. Clauss, G. Fischer, U. Hofmann, Surface properties of extremely thin graphite lamellae, in: Proc. Fifth Conf. Carbon, Elsevier, 1962, pp. 73–80.
[31] H.P. Böhm, W. Scholz, Vergleich der Darstellungsverfahren fur Graphitoxyd, Liebigs Ann. Chem. 691 (1965) 1–8.
[32] A.M. Dimiev, L.B. Alemany, J.M. Tour, Graphene oxide. Origin of acidity, its instability in water, and a new dynamic structural model, ACS Nano 7 (2013) 576–588.
[33] O.L. Blakslee, Elastic constants of compression-annealed pyrolytic graphite, J. Appl. Phys. 41 (1970) 3373.
[34] C. Lee, X. Wei, J.W. Kysar, J. Hone, Measurement of the elastic properties and intrinsic strength of monolayer graphene, Science 321 (2008) 385–388.
[35] U. Hofmann, E. König, Untersuchungen über Graphitoxyd, Z. Anorg. Allg. Chem. 234 (1937) 311–336.
[36] A.V. Talyzin, T. Hausmaninger, S. You, T. Szabó, The structure of graphene oxide membranes in liquid water, ethanol and water–ethanol mixtures, Nanoscale 6 (2014) 272–281.
[37] X. Fan, W. Peng, Y. Li, X. Li, S. Wang, G. Zhang, et al., Deoxygenation of exfoliated graphite oxide under alkaline conditions: a green route to graphene preparation, Adv. Mater. 20 (2008) 4490–4493.
[38] Q. Zheng, Z. Li, Y. Geng, S. Wang, J.-K. Kim, Molecular dynamics study of the effect of chemical functionalization on the elastic properties of graphene sheets, J. Nanosci. Nanotechnol. 10 (2010) 7070–7074.
[39] Q. Zheng, Y. Geng, S. Wang, Z. Li, J.-K. Kim, Effects of functional groups on the mechanical and wrinkling properties of graphene sheets, Carbon 48 (2010) 4315–4322.
[40] Q. Peng, L. Han, J. Lian, X. Wen, S. Liu, Z. Chen, et al., Mechanical degradation of graphene by epoxidation: insights from first-principles calculations, Phys. Chem. Chem. Phys. 17 (2015) 19484–19490.